Constraints on the effective mass splitting by the isoscalar giant quadrupole resonance

Jun Su ⬤,[*] Long Zhu, and Chenchen Guo

Sino-French Institute of Nuclear Engineering and Technology, Sun Yat-sen University, Zhuhai 519082, China

Background: Previous theoretical work has found that the effective mass of the nucleon influences the excitation energy of the isoscalar giant quadrupole resonance (ISGQR).

Purpose: The present paper presents an attempt to constrain the effective mass splitting by using the isospin dependence of the ISGQR energies.

Methods: Using the macroscopic Langevin equation (LE), the ISGQR energies are calculated from the particle density and kinetic energy density of the nucleus in the ground state, obtained from either the Thomas-Fermi (TF) approach or the Skyrme Hartree-Fock-Bogolyubov (SHFB) model.

Results: It is found that the calculations of the ISGQR energies by the SHFB+LE model agree with, or are even better than, the results by other approaches when applying the Skyrme functional Sly4. The values of the isoscalar and isovector effective masses are optimized by fitting the data for the ISGQR energies for a mass region from 28 to 238. The root-mean-squared deviation of the best fit to the data measured after the year 2000 is 0.22 MeV by the TF+LE model and 0.30 MeV by the SHFB+LE model. The extracted isoscalar effective mass is $0.70 < m_s^*/m < 0.73$. With respect to the isovector effective mass m_v^*, the constrained value is about half of the isoscalar effective mass m_s^*.

Conclusions: The present work supports the statement that, in neutron-rich matter, the effective mass of the neutron is definitely larger than that of the proton.

I. INTRODUCTION

The residual strong interactions between nucleons are of fundamental importance in understanding the nature of asymmetric nuclear objects including supernovae, neutron stars, and nuclei [1–4]. However, there still exist large uncertainties in our current knowledge. For decades the momentum-dependent potential has been predicted from microscopic calculations, such as the Dirac-Brueckner-Hartree-Fock model [5–7], the Skyrme-Hartree-Fock (SHF) model [8], and the relativistic mean-field model [9]. The concept of nonrelativistic effective mass m^* is used to parametrize the nonlocality of the single-particle potential [10,11]. Generally speaking the nucleon effective mass in symmetry nuclear media is generally determined ($m^*/m = 0.7 \pm 0.05$) at normal density and Fermi momentum [12–14]. However, the splitting of the effective masses between neutron and proton in asymmetric nuclear media has been a long-standing and controversial issue [15–18].

Many observables have been applied to constrain the effective mass. One of them is the isoscalar giant quadrupole resonance (ISGQR), which was discovered in the early 1970s [19,20]. So far, the ISGQR has been measured systematically over the nuclear mass range by using inelastic electron-scattering and light-ion-scattering experiments [21–31]. Because of the difficulty to produce targets of radioactivity nuclei, those measurements are limited to stable nuclei. Some new techniques, which were developed for measuring nuclear reactions at low momentum transfer in inverse kinematics, have been successfully used in the study of ISGQR [32,33]. In the future, those experimental methods can be applied to investigate the giant resonances of a large domain of isospin asymmetric nuclei, including unstable ones.

The ISGQR has been extensively studied in the past based on different theoretical models, such as the SHF model [34–36], the random-phase approximation (RPA) or its improved version the subtracted second random-phase approximation (SSRPA) [37,38], and the time-dependent Hartree-Fock model including pairing in the BCS approximation (TDHF + BCS) [39]. Those theoretical works support the hypothesis that the momentum-dependent part of the nuclear effective interaction strongly affects the ISGQR energy. In fact, efforts have been made to constrain neutron-proton effective-mass splitting based on the ISGQR data of several nuclei [40].

The present work is an attempt to investigate the effect of the effective-mass splitting on the ISGQR based on the systematic data. The paper is organized as follows: In Sec. II, we describe the method. In Sec. III, we present both the results and discussions. Finally, the summaries are given in Sec. IV.

---
*sujun3@mail.sysu.edu.cn

II. THEORETICAL FRAMEWORK

A. Langevin equation for isoscalar giant quadrupole resonance

When the velocity field can be described by a collective variable, the dynamic evolution of a nuclear system can be described by the Langevin equation for the collective variable, which is the fluid dynamic reduction of the Boltzmann-Langevin equation [41,42]. The ISGQR of a nuclei can be characterized by the collective variable

$$X = \sqrt{\frac{5}{16\pi}} \beta \cos \gamma, \qquad (1)$$

where the parameters β and γ are respectively the Hill and Wheeler coordinates in the spherical harmonics representation,

$$R(\theta, \varphi) = R_0 + R_0 \beta \cos \gamma Y_2^0(\theta, \varphi)$$
$$+ \frac{R_0}{\sqrt{2}} \beta \sin \gamma \left[Y_2^2(\theta, \varphi) + Y_2^{-2}(\theta, \varphi) \right], \qquad (2)$$

where R_0 is the radius of the sphere and Y_l^m is the spherical harmonic.

The Langevin equation for the collective variable X reads

$$\dddot{X} + \frac{1}{\tau}\ddot{X} + \frac{\Gamma}{M}\dot{X} + \frac{1}{M}\frac{\partial^2 V}{\partial X^2}\dot{X} + \frac{1}{\tau M}\frac{\partial V}{\partial X} = \frac{1}{M}\sqrt{\frac{\Gamma T}{\tau}} w(t), \qquad (3)$$

where M is the inertia parameter, Γ is the stiffness, τ is the relaxation time, V is the potential energy, and $w(t)$ is the random force. By applying the Skyrme energy density functional, one can express the inertia parameter M as [42]

$$M = 2m \int d^3\mathbf{r}\, r^2 \rho, \qquad (4)$$

and the stiffness Γ as

$$\Gamma = 8 \int d^3\mathbf{r} \left[\frac{\hbar^2}{2m}(\tau_n + \tau_p) + \varepsilon_{\text{eff}} \right],$$
$$\varepsilon_{\text{eff}} = \frac{1}{4}\left[t_1\left(1 + \frac{x_1}{2}\right) + t_2\left(1 + \frac{x_2}{2}\right) \right] \rho(\tau_n + \tau_p) \qquad (5)$$
$$+ \frac{1}{4}\left[t_2\left(x_2 + \frac{1}{2}\right) - t_1\left(x_1 + \frac{1}{2}\right) \right](\rho_n \tau_n + \rho_p \tau_p),$$

where $\tau_{n(p)}$ is the kinetic-energy density of the neutron (proton), and ε_{eff} is the momentum-dependent part of the potential-energy density. Considering the definition of the effective mass $m^*_{n(p)}$,

$$\frac{\hbar^2}{2m^*_{n(p)}} = \frac{\hbar^2}{2m} + \frac{1}{4}\left[t_1\left(1 + \frac{x_1}{2}\right) + t_2\left(1 + \frac{x_2}{2}\right) \right]\rho$$
$$+ \frac{1}{4}\left[t_2\left(x_2 + \frac{1}{2}\right) - t_1\left(x_1 + \frac{1}{2}\right) \right]\rho_{n(p)}, \qquad (6)$$

the stiffness Γ reads

$$\Gamma = 8 \int d^3\mathbf{r} \left(\frac{\hbar^2}{2m^*_n}\tau_n + \frac{\hbar^2}{2m^*_p}\tau_p \right). \qquad (7)$$

In Eq. (3), since the average value of the random force $w(t)$ is zero, it does not affect the excitation energy. In the GQR, the

volume of the system remains constant. Thus, the potential force arising from the density variation is much smaller than that due to the deformation of the Fermi surface [third term in Eq. (3)]. One can ignore the random force and the potential energy when calculating the excitation energy rather than the width of the resonance. In this case, the solution of the Langevin equation is

$$\dot{X}(t) = \dot{X}_0 e^{-t/2\tau} \cos\left(\sqrt{\frac{\Gamma}{M}} t + \varphi \right). \qquad (8)$$

The Fourier transform of the solution results in the excitation energy of the ISGQR,

$$E^* = \hbar\sqrt{\frac{\Gamma}{M}}. \qquad (9)$$

Equations (4), (7), and (9) provide a method to calculate the excitation energy of the ISGQR from the particle density and kinetic-energy density of the nucleus in the ground state. Meanwhile, one sees that the excitation energy of the ISGQR depends on the momentum-dependent part of the potential-energy density, and hence on the effective mass.

B. Excitation energy by the Thomas-Fermi approach

In the TF approximation, the kinetic-energy density can be expressed as a function of density. For the hard-sphere distribution at normal density, the integral in Eq. (7) can be calculated:

$$\Gamma_{hs} = \frac{24}{5} A \varepsilon_F \left[\frac{m}{m^*_n}\frac{(1+\delta)^{5/3}}{2} + \frac{m}{m^*_p}\frac{(1-\delta)^{5/3}}{2} \right], \qquad (10)$$

where ε_F is the Fermi energy at the normal density, $\delta = (N - Z)/A$ is the isospin asymmetry, which is calculated from the neutron number N, proton number Z, and mass number A of the nucleus. Unfortunately, the density of the nucleus is not the hard-sphere distribution, but with the surface arising from the density dispersion. Considering the surface effect, the stiffness Γ is assumed to be the product of Γ_{hs} and a factor f,

$$\Gamma = f \Gamma_{hs}. \qquad (11)$$

On the other hand, the inertia parameter M is expressed as

$$M = 2Am\langle r^2 \rangle, \qquad (12)$$

where $\langle r^2 \rangle$ is the mean-square radius of the nucleus, which can be taken from Refs. [43,44]. The root-mean-square charge radii are listed in Ref. [43]. Then the neutron radii can be calculated by using the empirical formula for the neutron skin [44].

The neutron (proton) effective mass m^*_n (m^*_p) in Eq. (10) can be expressed as a function of the isoscalar and isovector effective masses m^*_s and m^*_v,

$$\frac{1}{m^*_n} = \frac{1}{m^*_s} + \left(\frac{1}{m^*_s} - \frac{1}{m^*_v} \right)\delta,$$
$$\frac{1}{m^*_p} = \frac{1}{m^*_s} - \left(\frac{1}{m^*_s} - \frac{1}{m^*_v} \right)\delta. \qquad (13)$$

Substituting Eqs. (10)–(13) into Eq. (9), the square of the ISGQR energy can be expressed as

$$E^{*2} = \frac{12\hbar^2 \varepsilon_F}{5m\langle r^2 \rangle} \frac{fm}{m_s^*} \left[\left(1 + \delta - \frac{m_s^*}{m_v^*}\delta \right) \frac{(1+\delta)^{5/3}}{2} \right. $$
$$\left. + \left(1 - \delta + \frac{m_s^*}{m_v^*}\delta \right) \frac{(1-\delta)^{5/3}}{2} \right]. \quad (14)$$

Given the parameters fm/m_s^* and m_s^*/m_v^* further, one can calculate the excitation energy of the ISGQR. Let us note that Eq. (14) is deduced based on the macroscopic Langevin equation and the Thomas-Fermi approach. In the following, we call it "TF + LE" for short.

Equation (14) demonstrates the mass dependence of the ISGQR energy. As is well known, the radius of the nucleus is approximatively in direct proportion to $A^{1/3}$, where A is the mass number of the nucleus. Thus, one sees the approximate relation between the ISGQR energy and the mass number $E^* \propto A^{-1/3}$. More importantly, Eq. (14) shows that the isospin dependence of the ISGQR energy results from the isospin dependence of the radius, the effective-mass splitting, and the Fermi-surface splitting.

C. Excitation energy by Skyrme Hartree-Fock-Bogolyubov model

In fact, the Skyrme Hartree-Fock-Bogolyubov (SHFB) model [45] has been widely applied to study the nucleus in the ground state. In this case, one can perform the SHFB calculation and then consider Eqs. (4), (5), and (9), which provide a method to calculate the ISGQR energy from the properties of the nucleus in the ground state. Let us call this method "SHFB + LE" for short.
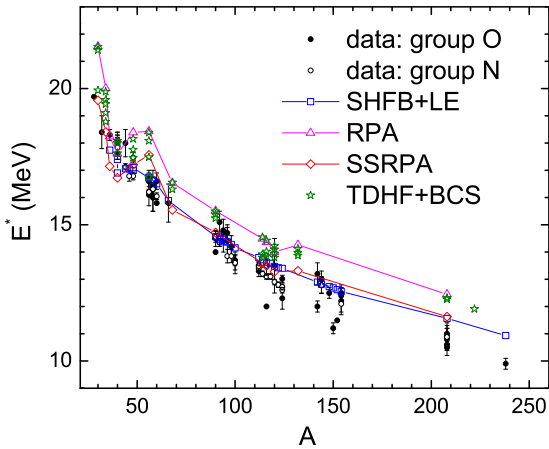

FIG. 1. Excitation energies of the ISGQR as a function of mass number. The calculations by the RPA (up triangles) and SSRPA (diamonds) models are taken from Ref. [38]. The calculations by the TDHF + BCS model (stars) are taken from Ref. [39]. In all calculations, the Skyrme force Sky4 is applied. Experimental data are taken from Refs. [21–32]. The data are divided into two groups: Group O includes those measured before the year 2000 and is shown as solid circles. Group N is for those measured after the year 2000 and is shown as open circles.

III. RESULTS AND DISCUSSIONS

A. Reliability of approaches

Let us test the reliability of the approach by comparing the predictions of the SHFB + LE model with the results of other approaches. The available data of ISGQR energies as well as the calculations by several models with the same functional Sky4 are shown in Fig. 1. The data are divided into two groups. Group O includes those measured before the year 2000 and is shown as solid circles. Group N is for those measured after the year 2000 and is shown as open circles. It is shown that the error bars for group O are generally larger than those for group N. Moreover, the values for ^{116}Sn in Group O are systematically deviated. With the development of the measuring technique, the data are more and more accurate and precise. The data show a $A^{-1/3}$ law. This is because the ISGQR energy is inversely proportional to the root-mean-square radius, while the radius of the stable nuclei is proportional to $A^{1/3}$.

Several models have been applied to calculate the mass dependence of the ISGQR energies. Although they are different types of approaches, the RPA and TDHF + BCS models provide calculations with agreement (as shown in Fig. 1). In comparison with the RPA model, the SSRPA model makes an important improvement and can provide calculations with better global agreement with the experimental data (see diamonds in Fig. 1). The SHFB + LE model reproduces the ISGQR energies globally but overestimates those of ^{208}Pb and ^{238}U, which is consistent with SSRPA model. In fact, the simple formula (9) is used to describe the ISGQR energies. However, the calculations agree with or are even better than the results of other approaches. An example can be seen for ^{56}Ni. The data and the calculation by our model for ^{56}Ni are about 16.5 MeV. But the calculations by the other three models are greater than 17 MeV and diverge from the $A^{-1/3}$ law.

The reliability of the TF + LE approach is also tested. The ISGQR energy cannot be calculated directly from Eq. (14) without the parameters fm/m_s^* and m_s^*/m_v^*. But one obtains an interesting proportional relationship by defining the weighted effective mass m_w^*:

$$E^{*2} \propto \frac{m}{m_w^*}, \quad \frac{m}{m_w^*} = \frac{m}{m_s^*} \left[\left(1 + \delta - \frac{m_s^*}{m_v^*}\delta \right) \frac{(1+\delta)^{5/3}}{2} \right.$$
$$\left. + \left(1 - \delta + \frac{m_s^*}{m_v^*}\delta \right) \frac{(1-\delta)^{5/3}}{2} \right]. \quad (15)$$

We test this proportional relationship for a given nucleus by performing the SHFB + LE calculations with thirty sets of Skyrme functionals, which are listed in Table I. The values of the incompressibility for the chosen functionals are about 230 MeV, which is the consensus reached by studying the isoscalar giant monopole resonance. The uncertainty of the symmetry energy is considered. The values of the symmetry energy at normal density S_0 for the chosen functionals are in the region from 28 to 32 MeV, meanwhile their slopes over density L are distributed from −0.31 to 70.31 MeV.

Figure 2 shows the correlation between the square of the ISGQR energy E^{*2} and the reciprocal of the weighted

TABLE I. The Skyrme functionals applied in this work, and the corresponding incompressibility K_0, symmetry energy S_0, slope of the symmetry energy over density L, and isoscalar and isovector effective masses (m_s^* and m_v^*) at normal density in symmetric nuclear matter.

	K_0 MeV	S_0 MeV	L MeV	$\frac{m_s^*}{m_0}$	$\frac{m_v^*}{m_0}$
SkMP	230.9	30	70.31	0.654	0.739
SLy9	229.8	32	54.86	0.666	0.572
SLy10	229.7	32	38.51	0.683	0.596
SLy7	229.7	32	46.94	0.689	0.605
SLy6	229.9	32	47.45	0.69	0.607
SLy4	229.9	32	45.94	0.694	0.612
SLy5	229.9	32	48.15	0.697	0.619
SKz4	230.1	32	5.75	0.7	0.554
SKz3	230.1	32	12.96	0.7	0.638
SKz2	230.1	32	16.81	0.7	0.781
SKz1	230.1	32	27.67	0.7	0.915
BSk9	231.3	30	38.29	0.8	0.717
BSk8	230.3	28	14.85	0.8	0.740
MSL0	230.0	30	60	0.8	0.934
BSk7	229.3	28	17.99	0.801	0.741
BSk6	229.1	28	16.84	0.801	0.750
SkS2	229.0	29	37.84	0.853	1.850
v110	231.2	28	7.51	1.05	1.004
MSk5	231.2	28	7.57	1.05	1.05
MSk2	231.6	30	33.35	1.05	1.05
MSk6	231.2	28	9.63	1.05	1.05
BSk1	231.3	28	7.19	1.05	1.05
MSk4	231.2	28	7.2	1.05	1.05
MSk7	231.2	28	9.4	1.05	1.05
v105	231.2	28	7.08	1.05	1.05
v100	231.2	28	8.73	1.05	1.105
v090	231.2	28	5.04	1.05	1.260
v080	231.2	28	2.23	1.05	1.524
v075	231.3	28	−0.31	1.05	1.750
MSk8	229.3	28	8.26	1.1	1.1

FIG. 2. Correlation between the square of the ISGQR energy and the reciprocal of the weighted effective mass for the nuclei ^{40}Ca, ^{90}Zr, and ^{208}Pb. The curves are linear fits. The data with the error bars are shown as gray.

GQR energies is significant when we extract the isoscalar mass from the ISGQR data.

B. Isospin dependence of ISGQR energies

One can fit the data to optimize the parameters by minimizing the root-mean-squared deviation σ as

$$\sigma^2 = \frac{\sum_i^{N_d} \left(\frac{E_i^{\text{calc}} - E_i^{\text{expt}}}{\sigma_i^{\text{expt}}} \right)^2}{\sum_i^{N_d} \left(\frac{1}{\sigma_i^{\text{expt}}} \right)^2}, \tag{16}$$

where E_i^{calc} and E_i^{expt} are the calculated and measured ISGQR energies, and σ_i^{expt} is the error of the data. The summation is for the number N_d of the data. In fact, the weight of each datum is not the same but depends on the error.

For the TF + LE model, the root-mean-squared deviations σ are plotted as a function of fitting parameters fm/m_s^* and m_s^*/m_v^*, as shown in Fig. 3. Since the data are divided into two groups (see Fig. 1), we fit the data in two groups. One sees from Fig. 1 that the error bars for the data in group N are generally smaller than those for group O. In this case, the value of the minimum root-mean-squared deviation 0.22 MeV by fitting to the data in group N is smaller than the value of 0.44 MeV for group O.

Considering that the root-mean-squared deviation is smaller than 0.22 MeV, the optimized parameters from Fig. 3(b) are $0.104 < fm/m_s^* < 0.106$ and $1.7 < m_s^*/m_v^* < 2.2$. From Eq. (14), one sees that the parameter fm/m_s^* relates the mass dependence of the ISGQR energies. Since there are data for a wide mass region, from 28 to 238, the uncertainty of the optimized parameter fm/m_s^* is quite small. The parameter m_s^*/m_v^* relates the isospin dependence of the ISGQR energies. Only the data for stable nuclei are available, thus the uncertainty in the optimized ratio m_s^*/m_v^* is huge. Moreover, the region of the optimized parameters for group N is narrower than that for group O. This phenomenon is also seen in Fig. 4.

effective mass m/m_w^* for the nuclei ^{40}Ca, ^{90}Zr, and ^{208}Pb. The good linear relationship between E^{*2} and m/m_w^* can be seen. The surface effect is neglected when we deduce the proportional relation between E^{*2} and m/m_w^*. The surface effect for light nuclei is more obvious than that for heavy nuclei. Thus, the linear relation for the heavy nucleus ^{208}Pb is better than that for the light nucleus ^{40}Ca. In addition, the slope for ^{208}Pb is smaller than that for ^{40}Ca. This is consistent with the fact that the ISGQR energy depends on the root-mean-square radius.

The calculated value of the ^{208}Pb nucleus is 10.56 MeV for the Skyrme force SKS2 ($m^*/m = 0.85$), and 11.00 MeV for the Skyrme force BSK9 ($m^*/m = 0.8$). Those calculations are in the region of the data (10.5–11.0 MeV). In fact, the earlier studies based on the RPA approach indicated the strong relation between the ISGQR energy and the effective mass. The literature suggests that the isoscalar mass is somewhere between 0.8 and 0.9 based on the data of the ISGQR energies for ^{208}Pb [46]. Our calculations support this finding. However, we show in the following that the isospin dependence of the
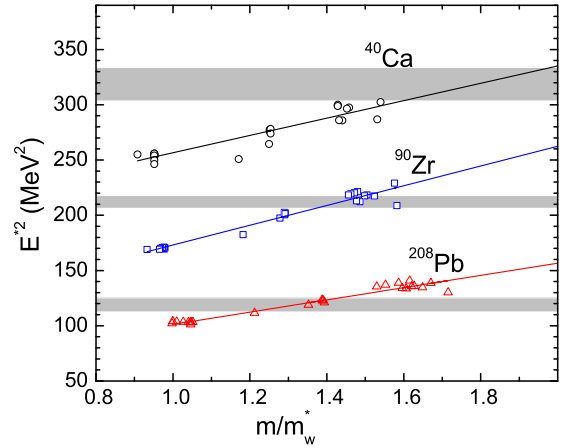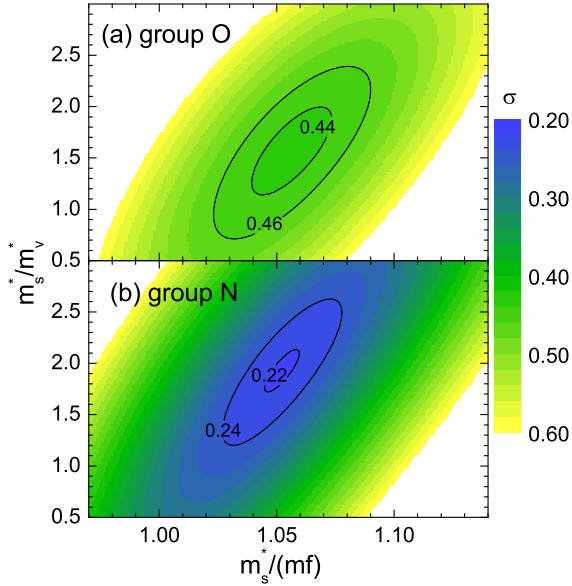
FIG. 3. A plot of the root-mean-squared deviations σ by TF + LE model as a function of fitting parameters fm/m_s^* and m_s^*/m_v^*. Panel (a) is the case to fit the data in group O and panel (b) is for group N.

Based on the Skyrme functional Sly4, we change the isoscalar and isovector effective masses and keep other parameters such as incompressibility, symmetry energy, and slope of the symmetry energy. In this case one can calculate the ISGQR energies by the SHFB + LE model and then the root-mean-squared deviations σ as a function of fitting parameters m_s^*/m and m_s^*/m_v^*. The results are shown in Fig. 4. There are two aspects for the surface effects on the ISGQR energies.
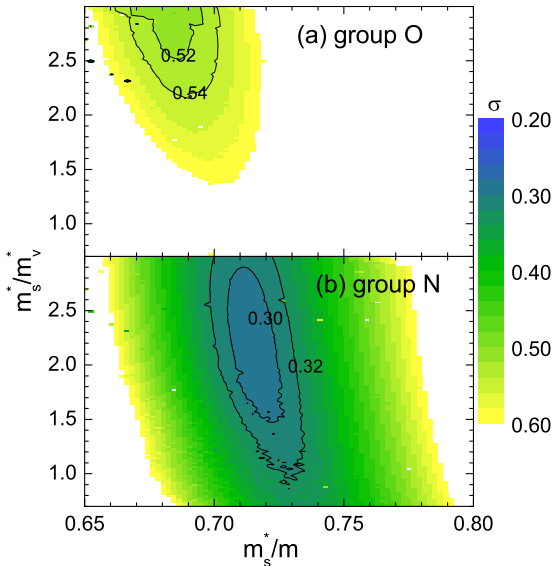

FIG. 4. A plot of the root-mean-squared deviations σ by SHFB + LE model as a function of fitting parameters m/m_s^* and m_s^*/m_v^*. Panel (a) is the fit the data in group O and panel (b) is for group N.

The first one arises from the density dispersion in the surface region of the nucleus. It affects the mass dependence of the ISGQR energies and has been expressed as the parameter f in Eq. (14). The second one is the contribution of the Fermi-surface splitting in the surface of the nucleus, which has been neglected and results in the $(1 \pm \delta)^{5/3}$ terms in Eq. (14). Those aspects of the surface effects are considered self-consistently by the SHFB model. However, one sees that the minimum of the root-mean-squared deviation by the SHFB + LE model is 0.30 MeV, which is larger than 0.22 MeV calculated by the TF + LE model.

Considering the root-mean-squared deviation smaller than 0.30 MeV in Fig. 4(b), the optimized isoscalar effective mass is about $0.70 < m_s^*/m < 0.73$. This restrained region agrees to the general determination $m_s^*/m = 0.7 \pm 0.05$ [12–14]. With respect to the isovector effective mass, the restrained region is $1.4 < m_s^*/m_v^* < 2.8$. In fact, the values of the effective-mass splitting were extracted by other observables, such as $(m_n^* - m_p^*)/m = (0.32 \pm 0.12)\delta$, which is obtained from the average of the nucleon isovector optical potentials [47], $(m_n^* - m_p^*)/m = (0.27 \pm 0.25)\delta$ based on the values of the symmetry energy and its density slope at normal density extracted from 28 different analyses [48], and $(m_n^* - m_p^*)/m = (0.41 \pm 0.15)\delta$ based on the data of nucleon-nucleus reaction and elastic angular differential cross sections [18]. The form of the effective-mass splitting used in the work is different from those in the earlier works. Furthermore, the extracted values here are much larger than the earlier values. However, those values agree that the effective mass of neutron is definitely larger than that of proton in neutron-rich matter.

It is worth giving a short discussion about the spherical symmetry, the surface effect, and the accuracy of the data. The approximation of the spherical symmetry is used in the model. But the deformation is obvious for some light nuclei. Moreover, the density in the surface of the nucleus is smaller than the normal density, which results in the smaller effective mass. The surface effect is more obvious in light nuclei. Last but not least, due the fine structure of the ISGQR, especially in light nuclei [49], the position of the ISGQR centroid is ambiguous. This behavior contributes to the error of the data. Generally, the isospin asymmetry of the light stable nuclei is smaller than that of the heavy stable nuclei. Thus, more data for the heavy and spherical nuclei are beneficial for the pertinent method. It is interesting to study the above three effects for the light nuclei, which is a work in progress.

IV. CONCLUSION

In summary, thanks to the macroscopic Langevin equation (LE), the excitation energies of the isoscalar giant quadrupole resonance (ISGQR) are calculated from the particle density and kinetic-energy density of the nucleus in the ground state, which can be provided by the Thomas-Fermi (TF) approach or the Skyrme Hartree-Fock-Bogolyubov (SHFB) model. Based on the TF + LE approach, the weighted effective mass is defined and demonstrated to be inversely proportional to square of the ISGQR energy. This proportional relation for a given nucleus is obtained by performing the SHFB + LE calculations with thirty sets of Skyrme functionals. The

reliability of the SHFB + LE approach is tested by comparing the predictions with the results of other theoretical approaches describing the ISGQR.

The effective mass in ^{208}Pb constrained by the SHFB + LE model is 0.8, which supports the literature suggesting tht the isoscalar mass is somewhere between 0.8 and 0.9 [46]. Furthermore, by comparing the calculations to the existing data, the effects of the isoscalar and isovector effective masses at normal density are investigated. With consideration of the accuracy and precision, only the ISGQR energy data measured after the year 2000 are considered. The extracted isoscalar effective mass is $0.70 < m_s^*/m < 0.73$, which is consistent with the general determination 0.7 ± 0.05 [12–14]. With respect to the isovector effective mass, the restrained region is $1.7 < m_s^*/m_v^* < 2.2$ by the TF + LE approach, and $1.4 < m_s^*/m_v^* < 2.8$ by the SHFB + LE approach. Recently,

new techniques developed for measuring nuclear reactions at low momentum transfer in inverse kinematics were successfully used to study isoscalar giant resonances [32,33]. In the near future those experimental methods will be applied to investigate the ISGQR of a large domain of neutron-rich nuclei. The method in this work can be applied to analyze those data and improve our knowledge of the effective-mass splitting.

ACKNOWLEDGMENTS

[1] N. Bohr, Nature (London) **137**, 344 (1936).

[2] P. Danielewicz, Science **298**, 1592 (2002).

[3] C. Fuchs and H. H. Wolter, Eur. Phys. J. A **30**, 5 (2006).

[4] G. Giuliani, H. Zheng, and A. Bonasera, Prog. Part. Nucl. Phys. **76**, 116 (2014).

[5] E. N. E. van Dalen, C. Fuchs, and A. Faessler, Phys. Rev. Lett. **95**, 022302 (2005).

[6] W. Zuo, L. G. Cao, B. A. Li, U. Lombardo, and C. W. Shen, Phys. Rev. C **72**, 014005 (2005).

[7] F. Sammarruca, Int. J. Mod. Phys. E **19**, 1259 (2010).

[8] L. Ou, Z. Li, Y. Zhang, and M. Liu, Phys. Lett. B **697**, 246 (2011).

[9] L.-W. Chen, C. M. Ko, and B.-A. Li, Phys. Rev. C **76**, 054316 (2007).

[10] M. Prakash, J. Wambach, and Z. Ma, Phys. Lett. B **128**, 141 (1983).

[11] S. Shlomo and J. Natowitz, Phys. Lett. B **252**, 187 (1990).

[12] A. Steiner, M. Prakash, J. Lattimer, and P. Ellis, Phys. Rep. **411**, 325 (2005).

[13] B. LI, L. Chen, and C. Ko, Phys. Rep. **464**, 113 (2008).

[14] V. Baran, M. Colonna, V. Greco, and M. Ditoro, Phys. Rep. **410**, 335 (2005).

[15] J. W. Negele and K. Yazaki, Phys. Rev. Lett. **47**, 71 (1981).

[16] Y. Zhang, M. Tsang, Z. Li, and H. Liu, Phys. Lett. B **732**, 186 (2014).

[17] W.-J. Xie and F.-S. Zhang, Phys. Lett. B **735**, 250 (2014).

[18] X.-H. Li, W.-J. Guo, B.-A. Li, L.-W. Chen, F. J. Fattoyev, and W. G. Newton, Phys. Lett. B **743**, 408 (2015).

[19] R. Pitthan and T. Walcher, Phys. Lett. B **36**, 563 (1971).

[20] S. Fukuda and Y. Torizuka, Phys. Rev. Lett. **29**, 1109 (1972).

[21] F. E. Bertrand, Nucl. Phys. A **354**, 129 (1981).

[22] D. H. Youngblood, Y.-W. Lui, H. L. Clark, B. John, Y. Tokimoto, and X. Chen, Phys. Rev. C **69**, 034315 (2004).

[23] Y.-W. Lui, D. H. Youngblood, Y. Tokimoto, H. L. Clark, and B. John, Phys. Rev. C **70**, 014307 (2004).

[24] Y.-W. Lui, D. H. Youngblood, H. L. Clark, Y. Tokimoto, and B. John, Phys. Rev. C **73**, 014314 (2006).

[25] Y. Tokimoto, Y.-W. Lui, H. L. Clark, B. John, X. Chen, and D. H. Youngblood, Phys. Rev. C **74**, 044308 (2006).

[26] B. Nayak, U. Garg, M. Hedden, M. Koss, T. Li, Y. Liu, P. M. Rao, S. Zhu, M. Itoh, H. Sakaguchi et al., Phys. Lett. B **637**, 43 (2006).

[27] T. Li, U. Garg, Y. Liu, R. Marks, B. K. Nayak, P. V. Madhusudhana Rao, M. Fujiwara, H. Hashimoto, K. Nakanishi, S. Okumura et al., Phys. Rev. C **81**, 034309 (2010).

[28] Y.-W. Lui, D. H. Youngblood, S. Shlomo, X. Chen, Y. Tokimoto, Krishichayan, M. Anders, and J. Button, Phys. Rev. C **83**, 044327 (2011).

[29] Krishichayan, Y.-W. Lui, J. Button, D. H. Youngblood, G. Bonasera, and S. Shlomo, Phys. Rev. C **92**, 044323 (2015).

[30] D. H. Youngblood, Y.-W. Lui, Krishichayan, J. Button, G. Bonasera, and S. Shlomo, Phys. Rev. C **92**, 014318 (2015).

[31] J. Button, Y.-W. Lui, D. H. Youngblood, X. Chen, G. Bonasera, and S. Shlomo, Phys. Rev. C **96**, 054330 (2017).

[32] C. Monrozeau, E. Khan, Y. Blumenfeld, C. E. Demonchy, W. Mittig, P. Roussel-Chomaz, D. Beaumel, M. Caamaño, D. Cortina-Gil, J. P. Ebran et al., Phys. Rev. Lett. **100**, 042501 (2008).

[33] J. Zamora, T. Aumann, S. Bagchi, S. Bönig, M. Csatlós, I. Dillmann, C. Dimopoulou, P. Egelhof, V. Eremin, T. Furuno et al., Phys. Lett. B **763**, 16 (2016).

[34] O. Bohigas, A. Lane, and J. Martorell, Phys. Rep. **51**, 267 (1979).

[35] E. Lipparini and S. Stringari, Phys. Rep. **175**, 103 (1989).

[36] P. Gleissl, M. Brack, J. Meyer, and P. Quentin, Ann. Phys. (NY) **197**, 205 (1990).

[37] J. Blaizot, Phys. Rep. **64**, 171 (1980).

[38] O. Vasseur, D. Gambacurta, and M. Grasso, Phys. Rev. C **98**, 044313 (2018).

[39] G. Scamps and D. Lacroix, Phys. Rev. C **88**, 044310 (2013).

[40] H.-Y. Kong, J. Xu, L.-W. Chen, B.-A. Li, and Y.-G. Ma, Phys. Rev. C **95**, 034324 (2017).

[41] S. Ayik, E. Suraud, J. Stryjewski, and M. Belkacem, Z. Phys. A: Atomic Nucl. **337**, 413 (1990).

[42] D. Boilley, Y. Abe, S. Ayik, and E. Suraud, Z. Phys. A: Hadrons Nucl. **349**, 119 (1994).

[43] I. Angeli and K. Marinova, At. Data Nucl. Data Tables **99**, 69 (2013).

[44] A. Trzcińska, J. Jastrzębski, P. Lubiński, F. J. Hartmann, R. Schmidt, T. von Egidy, and B. Kłos, Phys. Rev. Lett. **87**, 082501 (2001).

[45] K. Bennaceur and J. Dobaczewski, Comput. Phys. Commun. **168**, 96 (2005).

[46] P. Klupfel, P.-G. Reinhard, T. J. Burvenich, and J. A. Maruhn, Phys. Rev. C **79**, 034310 (2009).

[47] C. Xu, B.-A. Li, and L.-W. Chen, Phys. Rev. C **82**, 054607 (2010).

[48] B.-A. Li and X. Han, Phys. Lett. B **727**, 276 (2013).

[49] C. Kureba, Z. Buthelezi, J. Carter, G. Cooper, R. Fearick, S. Förtsch, M. Jingo, W. Kleinig, A. Krugmann, A. Krumbolz *et al.*, Phys. Lett. B **779**, 269 (2018).